Quantifying urban heat island effects and human comfort for cities of variable size and urban morphology in the Netherlands

G. J. Steeneveld,[1] S. Koopmans,[1] B. G. Heusinkveld,[1] L. W. A. van Hove,[1] and A. A. M. Holtslag[1]

Received 23 March 2011; revised 11 August 2011; accepted 15 August 2011; published 29 October 2011.

[1] This paper reports on the canopy layer urban heat island (UHI) and human comfort in a range of small to large cities and villages in the Netherlands. To date, this subject has not been substantially studied in the Netherlands, since it has a relatively mild oceanic (Cfb) climate and impact was assumed to be minor. To fill this knowledge gap, this paper reports on observations of a selected network of reliable hobby meteorologists, including several in The Hague and Rotterdam. A number of alternative measures were also used to quantify UHI, i.e., the generalized extreme value distribution and return periods of UHI and adverse human comfort; its uncertainties were estimated by the statistical method of bootstrapping. It appeared essential to distinguish observations made at roof level from those made within the urban canyon, since the latter related more closely to exposure at pedestrian level and to urban canyon properties in their close neighborhood. The results show that most Dutch cities experience a substantial UHI, i.e., a mean daily maximum UHI of 2.3 K and a 95 percentile of 5.3 K, and that all cities experience a shadow effect in the morning when cities remain cooler than the rural surroundings. Also, an evident relation between the median of the daily maximum UHI and its 95 percentile was discovered. Furthermore, the 95 percentile of the UHI appears well correlated with population density. In addition, we find a significant decrease of UHI and the percentage of surface area covered by green vegetation, but the relation with open water remains unclear.

Citation: Steeneveld, G. J., S. Koopmans, B. G. Heusinkveld, L. W. A. van Hove, and A. A. M. Holtslag (2011), Quantifying urban heat island effects and human comfort for cities of variable size and urban morphology in the Netherlands, *J. Geophys. Res.*, *116*, D20129, doi:10.1029/2011JD015988.

1. Introduction

[2] Human population in cities and urban areas has increased markedly from 29% of the global population in 1950 to 49% in 2005. Urbanization is projected to increase even further to ~60% in 2030 [*United Nations*, 2005]. Although several motivations exist for migration toward cities, e.g., education, entertainment, housing, minimization of transportation, or health care access, the most dominant reason is the economic opportunities that are available in urban regions. One consequence of increased urbanization is a greater interest in urban meteorology, since it governs the environmental quality (in terms of thermodynamics and atmospheric chemistry) of human living and working areas. A better scientific understanding of the physics of urban environmental meteorology may help optimize urban planning to prevent the occurrence of local meteorological conditions that are adverse to human populations [*Dieleman et al.*, 2002; *Svensson and Eliasson*, 2002; *Dimoudi and Nikolopoulou*, 2003; *Vonk et al.*, 2007, *Coutts et al.*, 2008; *Mills*, 2009; *Reid et al.*, 2009].

[3] Urban areas experience a substantially different meteorology than their rural counterparts [*Oke*, 1982; *Godowitch et al.*, 1985]. The physical properties of cities and buildings result in a modified surface radiation and energy budget, which need to be accounted for in modeling studies [*Grimmond et al.*, 2010, 2011]. First, building clusters interact with solar radiation such that multiple reflections between buildings and roads occur before the solar radiation is reflected to space. Therefore, cities typically have a smaller albedo than crops or grasses. In addition, buildings limit the sky view of the surface, and therefore emission of thermal radiation to space is limited. It is evident that the aspect ratio of building height to road width is a governing parameter for the sky view [*Svensson*, 2004; *Ali-Toudert and Mayer*, 2006; *Kanda*, 2007]. Also, building configurations provide additional friction to the flow, which affects wind speed and turbulence intensity not only in the cities, but also downstream from them. Moreover, fabric, concrete and asphalt have a higher heat capacity than rural areas, which limits rapid cooling after the evening transition. Finally, anthropogenic activities result in a significant [*Hinkel and Nelson*, 2007], but currently poorly quantified, heat emission [*Souch and Grimmond*, 2006; *Krpo et al.*, 2010].

[1]Meteorology and Air Quality Section, Wageningen University, Wageningen, Netherlands.

0148-0227/11/2011JD015988

[4] Altogether, these properties result in the formation of a so-called urban boundary layer. Especially the daytime heat storage in buildings and the subsequent heat release after sunset results in a canyon layer urban heat island: the temperature at pedestrian level is higher than in the rural neighborhood. During warm summer periods, these special meteorological properties can be significant for vulnerable groups, e.g., the elderly, young children, and people with cardiovascular diseases [*Wang et al.*, 2009; *Reid et al.*, 2009]. In addition, the city temperature affects outdoor working conditions and productivity. Also, the urban microclimate causes plants to flower earlier than in the countryside, which may trigger hay fever earlier than in the countryside as well [*Mimet et al.*, 2009]. Hence, on-time warning of vulnerable groups could limit adverse effects and improve their thermal comfort [*Lenzuni et al.*, 2009]. For such alerts to be done effectively, understanding and quantification of urban meteorology is required.

[5] Recognizing the conceptual framework of different scale levels of the urban atmosphere, as defined by the urban boundary layer, the urban surface layer, and the urban canopy layer, the aim of this study is to quantify the canopy layer urban heat island (UHI) [*Oke*, 1976] in the Netherlands based on observations by a network of hobby meteorologists. We relate the UHI effect to such urban morphological parameters as the amount of green cover, presence of water bodies, and population densities. For the selected sites, human comfort will also be quantified and compared. The multiple motivations to study urban meteorology for Dutch cities in particular are as follows. First, until recently, the UHI was hypothesized to be relatively small and unimportant, since the Netherlands is located in a mild climate of the Cfb type [*Köppen*, 1931], close to the sea. The Cfb climate class covers the maritime temperate climates, which are dominated by the polar front, leading to variable, often overcast weather. In the Cfb climate, summers are generally cool because of cloud cover, and winters are milder than in other climates at similar latitudes. Information regarding the Dutch UHI is virtually nonexistent, from both observational and modeling perspectives. Second, a large part of the Netherlands is located below sea level, and water levels in canals and ditches are artificially maintained at a high level. Dutch cities are known for their high density of canals, and one can hypothesize that this special feature may influence the UHI [*Xu et al.*, 2010], which might therefore differ from other (European) cities. Finally, the Netherlands, and especially the western part, is densely populated, with 398 and 918 inhabitants per square kilometer, respectively, and is ranked 27 out of 236 countries in population density. As such, a high potential exists for adverse effects on human comfort.

[6] Furthermore, one may hypothesize that the projected climate change will also affect liveability, and particularly human comfort in Dutch cities. Hence, adaptation and mitigation measures might be initiated to minimize the adverse effects [*Takebayashi and Moriyama*, 2009]. Such measures can range from modification of city design strategy and building material and introduction of vegetation (e.g., on roofs) in cities [*Synnefa et al.*, 2008; *Mills*, 2009]. However, before starting these activities, the quantification of a baseline for UHI and heat stress is required.

[7] Apart from the use of hobby meteorological data, this study introduces a number of innovative analysis methods for UHI and human comfort quantification (from observational and modeling perspective). These cover return periods of daily maximum UHI values, daily maximum human comfort values, as well as their uncertainties by applying the statistical bootstrapping method.

2. Material and Methods

2.1. Available Observations

[8] Because of the lack of attention to urban meteorology during the last decade, observations of the UHI are scarce for the Netherlands. *Floor* [1970] and *Conrads* [1975] report a field campaign on the urban climate of Utrecht (~60 km from the coast), where they recorded a UHI of ~7 K for warm summer days. Despite this large UHI and typical Dutch moist land surface conditions, more research was not performed until recently, when *Heusinkveld et al.* [2010] found a UHI of ~8 K and ~7 K for Rotterdam and Arnhem (a relatively small city ~150 km inland), respectively, using mobile measurement devices (i.e., bicycles).

[9] The nature of the city makes it difficult to set up instrumentation that follows the World Meteorological Organization (WMO) guidelines for rural terrain. WMO guidelines for urban meteorological observations have only been available since 2006 [*Oke*, 2006]. For these reasons, we decided to use observations by Dutch hobby meteorologists (Table 1 and Figure 1a). Also, hobby meteorological data offer the possibility to study long-term records rather than being limited to data from a few intensive observational campaigns that are usually undertaken in warm summer episodes. These stations have been selected on the basis of the available record length and on city size, because we intend to include both small and large cities (10^3–10^6 inhabitants). Figure 1 shows that our observations cover the northern part of the country rather well, but observations are lacking in the south, apart from the city of Tilburg. On the other hand, the majority of the largest cities in the western part, i.e., Rotterdam, Delft, The Hague (and its suburbs), Leiden, and Haarlem have been included. This part of the country is known as the "Randstad" and is the most densely populated region, as well as the most humid part of the country.

[10] In addition to the hobby meteorological stations, observations from three weather stations operated by Wageningen University are available within the Rotterdam metropolis (Figure 1b). The three stations, labeled as Rotterdam-Center, -East, and -South, have been sited such that they represent different urban morphologies and green vegetation cover within the city. Thus, we can learn about variability of the UHI and human comfort within the city, which is one of the cutting-edge problems in urban meteorology [e.g., *Dandou et al.*, 2005]. The station in Rotterdam-Center represents a densely built commercial area, while the eastern and southern stations represent relatively green suburban residential and densely built up residential neighborhoods, respectively.

[11] A reliable data analysis of the recorded observations requires an assessment of the quality of the observations by hobby meteorologists. The assessment must address both instrumental issues and possible adverse effects of the local setup of the instrumentation. Since a long-term, on-site intercomparison for all utilized equipment is virtually impossible, we are constrained by the uncertainties reported

Table 1. Characteristics of Hobby Meteorological Stations

No.	City	Lat, Long (deg)	Number of Inhabitants per 1000	Start Date	End Date	Number of Sampled Days	System	Measurement Elevation (m)	Ventilation[a]
				Urban Canyon Stations					
1	Rotterdam	51.917, 4.43	588	12/2007	03/2009	254	LaCrosse	9	
2	Rotterdam-Center	51.9253, 4.468	588	09/2009	09/2010	309	Campbell	3	YN
3	Rotterdam-East	51.9257, 4.488	588	09/2009	09/2010	226	Campbell	3	YN
4	Rotterdam-South	51.887, 4.548	588	09/2009	09/2010	211	Campbell	1.5	YN
5	The Hague	52.04, 4.24	483	07/2007	04/2009	600	Davis Vantage Pro+	1.5	YF
6	Delft	51.98, 4.34	97	01/2007	03/2009	806	LaCrosse	1.5	YF
7	Haarlem	52.37, 4.66	149	12/2005	02/2008	249	Ultimeter 2000	1.5	YN
8	Purmerend	52.49, 4.93	79	01/2008	03/2009	708	WS2350	1.5	N
9	Leeuwarden	53.206, 5.810	94	01/2007	03/2009	747	Davis Vantage Pro 2 +	3	YN
10	Apeldoorn	52.200, 5.933	136	01/2008	06/2009	522	WMR918	1.5	YN
11	Wageningen	51.97, 5.67	35	01/2008	07/2010	826	Oregon Scientific WMR-200	1.5	N
12	Heemskerk	52.499, 4.683	39	01/2005	12/2008	1437	Weather-monitor II	1.5	YN
13	Heerhugowaard	52.670, 4.847	50	01/2005	04/2009	1535	Davis Vantage Pro 2	1.5	YF
14	Leiden	52.162, 4.540	117	03/2004	03/2009	1978	LaCrosse WS 3600	1.5	YN
15	Doornenburg	51.890, 6.00	2.7	06/2007	06/2009	737	Vantage Pro	3.5	YN
16	Losser	52.255, 7.00	23	01/2003	12/2008	2167	Vantage Pro	3.8	YN
17	Damwoude	53.291, 5.978	5.5	01/2005	04/2009	1536	Vantage pro2+ 24-h FARS	3	YF
18	Ijsselmuiden	52.570, 5.928	12	07/2005	07/2009	1417	WS2305	1.5	YF
19	Groningen	53.216, 6.567	198	01/1999	03/2009	1823	Davis WM-2	1.5	N
20	IJsselmonde	51.881, 4.526	61	02/2008	10/2010	728	Ultimeter 2100	1.5	N
21	Tilburg	51.553, 5.095	204	08/2009	10/2010	435	Cresta WXR815LM	1.5	YN
				Roof Stations					
22	Houten	52.033, 5.166	47	07/2006	04/2009	959	Davis Vantage Pro 2	1.5	YF
23	Voorburg	52.08, 4.35	40	01/2006	12/2008	1072	Davis Vantage Pro	14	YN
24	Assen	53.01, 6.568	65	01/2007	03/2009	769	Davis Vantage Pro 2	12	YN
25	Gouda	52.011, 4.706	71	06/2006	11/2009	1214	Davis Vantage Pro 2	12	YN
26	Rijnmond	51.875, 4.467	12	05/2006	10/2010	1631	Davis Vantage Pro 2	30	N
27	Capelle a/d IJssel	51.950, 4.571	65	02/2008	10/2010	966	Davis Vantage Pro2+ 24hr	9.5	YN

No.	Degree of Shadowing	KNMI Reference Station (Label, Figure 1)	Distance Urban-Rural (km)	Green Cover (%)	Water Cover (%)	Sky View Factor[b]	Local Climate Zone[c]
		Urban Canyon Stations					
1	Negligible; shielded	Rotterdam AP (A)	4.1	8.3	9.0	0.68	*CHR*
2	Inner city station close to building; shielded	WUR ref station (Aw)	7.5	4.9	1.0	0.74	*CHR*
3	Roof station; shielded	WUR ref station (Aw)	10.3	12.8	8.5	0.6	*OLR*
4	Shielded	WUR ref station (Aw)	11.7	5.5	1.0	0.90	*CMR*
5	5 h; shielded	Valkenburg (B)	17.3	22.8	2.7	0.81	*OLR*
6	Shielded	Rotterdam AP (A)	8.2	31.7	2.1	0.75	*OLR*
7	Not much; shielded	Schiphol (C)	9.4	17.2	3.2	0.74	*CLR*
8	Exposed to sun until noon in summer; shielded	Berkhout (D)	15.9	40.0	1.3	0.71	*OLR*
9	Completely, north side; shielded	Leeuwarden AP (E)	2.3	33.7	0.9	0.71	*ELR*
10	Not shadowed	Deelen (G)	18.7	23.6	0.3	0.93	*OLR*
11	Completely; shielded	Wageningen Univ. (F)	1.5	20.6	2.6	0.82	*CLR*
12	Shielded	Schiphol (C)	17.8	32.5	1.7	0.67	*CLR*
13	Early morning and late evening; shielded	Berkhout (D)	11.3	32.1	1.9	0.71	*OLR*
14	Completely, north side; no radiation shield	Schiphol AP (C)	26.7	3.6	4.5	0.75	*CLR*
15	Shielded	Deelen (G)	20.3	43.8	0.7	0.82	*OLR*
16	Shielded	Twente (H)	8.0	21.0	0.1	0.82	*OLR*
17	Exposed to sun early morning and evening; shielded	Leeuwarden AP (E)	18.3	56.1	0.6	0.75	*ELR*
18	Afternoon (3/5) negligible; shielded	Heino (I)	24.3	15.3	10.4	0.75	*OLR*
19	In shadow in afternoon	Eelde (J)	13.1	23.4	2.2	0.71	*OLR*
20	Radiation shield present	Rotterdam AP (A)	11.1	13.0	6.5	0.71	*CMR*
21	Garden; shielded station	Gilze-Rijen (K)	10.1	46.6	0.5	0.7	*CLR*
		Roof Stations					
22	Negligible; shielded	De Bilt (L)	7.6	33.2	1.1		*OLR*
23	Negligible; shielded	Rotterdam AP (A)	13.8	15.7	2.0		*CLR*
24	Negligible; shielded	Eelde (J)	13.8	17.7	3.2		*OMR*
25	Roof; shielded station	Cabauw (M)	15.9	9.5	4.3		*CLR*
26	Balcony apartment; shielded	Rotterdam AP (A)	9.9	20.1	11.5		*OHR*
27	Negligible, roof station	Rotterdam AP (A)	7.9	7.7	7.4		*CLR*

[a]Ventilation: N, none; YN, natural; YF, forced ventilation.
[b]Sky view factor estimated from building height and street width from the Dutch Digital Elevation Model (http://www.ahn.nl).
[c]Local climate zone as in the work by *Stewart and Oke* [2010]: CHR, compact high rise; OLR, open-set low rise; CLR, compact low rise; ELR, extensive low rise; OMR, open-set mid rise; OHR, open-set high rise.

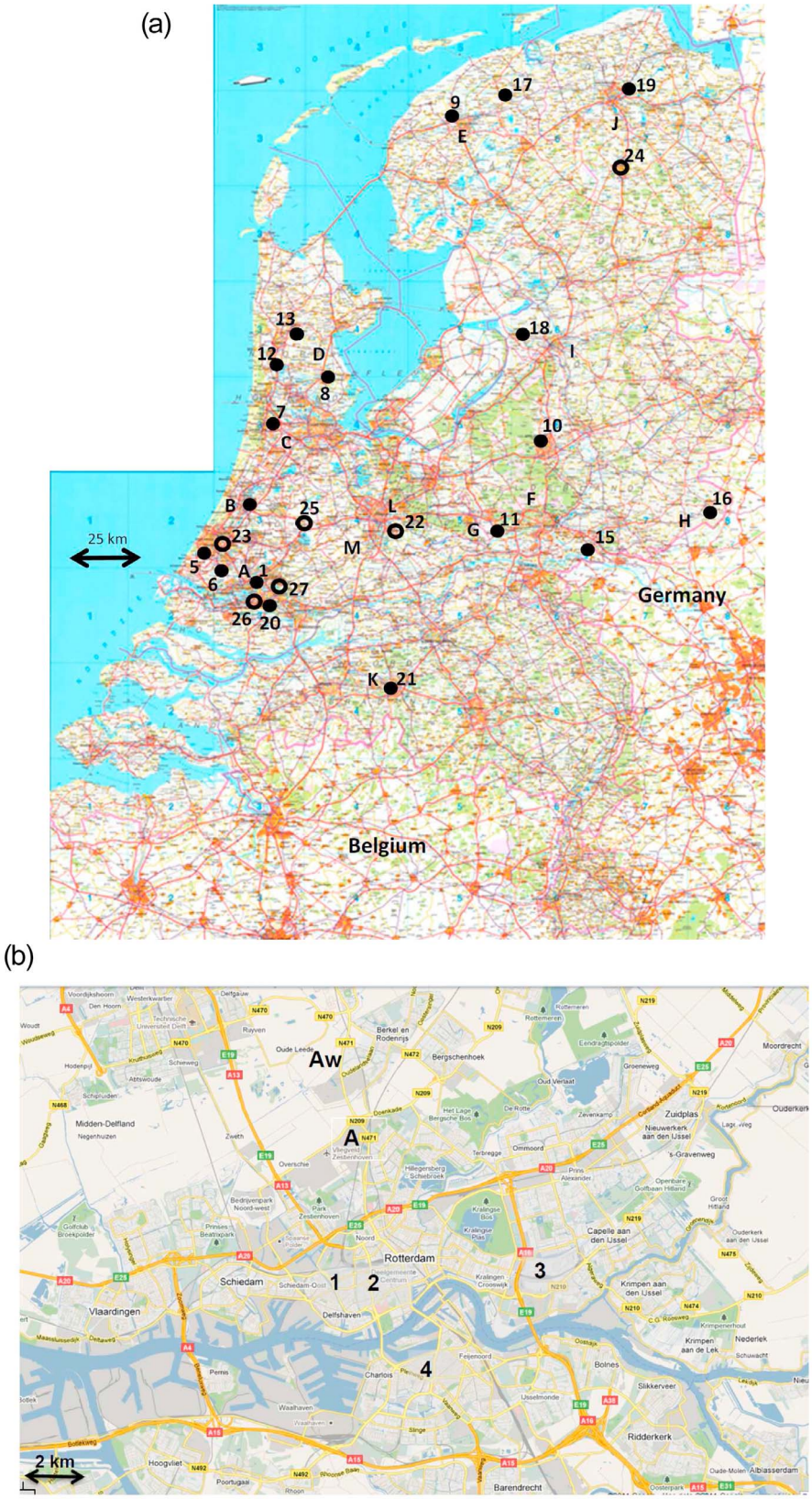

Figure 1. (a) Map of the Netherlands with locations with available hobby meteorological observations (filled circles) and reference station (characters). Country borders are indicated by the pink polygons. Characters and numbers refer to Table 1. (b) Map of observational network in Rotterdam, in which the label prefixes A and N indicate highway and regional roads, respectively.

Table 2. Measurement Accuracy for Reference and Hobby Meteorological Stations

Weather Station	T (K)	RH (%)	U ($m\ s^{-1}$)
Hobby stations			
Cresta WXR-815	1	5	0.9
LaCrosse WS2350	0.1	1	0.1
Weathermonitor2	0.5	3	1 $m\ s^{-1}$ or 5% of U
Ultimeter2000	0.5	4	0.9
Oregon Sci WMR918	1	4	1 $m\ s^{-1}$ or 5% of U
Vantage Pro+ 2	0.5	3	1
Reference stations			
KNMI ref. station	0.1	3	0.5 $m\ s^{-1}$ for $U < 5\ m\ s^{-1}$, ±10% for $U > 5\ m\ s^{-1}$
WUR ref. station	0.3	2	0.5 $m\ s^{-1}$

by the manufacturers. Table 2 lists the typical uncertainties for the variables deduced from the hobby meteorological stations used in this study, as well as uncertainties for the reference stations. The difference in accuracy among the systems is relatively small, with typical uncertainties of 0.5 K, 4%, and 1 ms^{-1} for temperature, relative humidity, and wind speed, respectively. As a reference, the Dutch National Weather (KNMI) service reports 0.1 K, 3%, and 0.5 ms^{-1} for the uncertainties in the selected rural reference stations. For the Wageningen University (WUR) weather stations, we assume measurement uncertainties are approximately similar to those reported by KNMI.

[12] Concerning the instrumental setup, Table 1 distinguishes between stations in the urban canyon and stations at roof (and balcony) level. The observations in the latter category might not follow the concept of the urban canyon layer completely, and their interpretation is possibly less straightforward; therefore, they will be analyzed separately. Most instruments are located in gardens and are well ventilated and shielded. A few stations lack ventilation or a radiation shield, which can in principle introduce nonhomogeneity in the data set. Since the timing of the recorded UHI will be influenced by the time at which the surroundings of the instrument experience direct solar radiation, the typical hours of shadowing are listed as well. Several hobby meteorological stations were removed from the current analysis because they showed unphysical behavior in the timing of the maximum UHI (e.g., in the morning several hours after sunrise).

[13] In terms of detection of UHI, *Sakakibara and Owa* [2005] report that the estimated UHI depends substantially on the choice of the rural reference station. These authors note that to obtain an accurate estimate of the UHI of a coastal city, the UHI should be determined using a reference station that is at the same distance from the sea as the city under consideration. Also, *Runnalls and Oke* [2000] also report that the greatest potential for errors in estimated UHI results from the selected reference station. For coastal cities, different advection rates may affect the recorded UHI. Since the Netherlands is a coastal region, it is important to realize and to account for this potential source of error (see also section 2.2).

[14] Our analysis should account for how elevation differences between hobby meteorological stations and their reference stations may influence the estimated UHI. Because the Netherlands is relatively flat, the applied temperature corrections, assuming a dry adiabatic lapse rate, are on average rather small (median value of 0.04 K), but not negligible, for Apeldoorn (0.32 K), Rotterdam-Rijnmond (0.34 K), and Doornenburg (0.39 K). For the latter, it should be mentioned that it is relatively far from its rural reference station (Deelen), and the typical land use and soil types differ substantially (clay in Doornenburg and sandy soil in Deelen).

[15] In the Netherlands, a relatively large UHI may occur when fog, either radiation fog in the relatively flat and humid polder regions or from advection fog from the North Sea or Lake IJssel, occurs at one of the two stations that are required to determine the UHI. *Conrads* [1975] reports a UHI of ~6 K for Amsterdam during a morning when fog was present in the countryside but absent in the city. Because our research focus is on the radiation-driven UHI in the context of human comfort and not on other processes that might trigger a UHI, we excluded all observations with a relative humidity (RH) equal to or larger than 99%. In addition, time slots in which the maximum daily UHI was reported but that coincided with precipitation during in the same hour were rejected from the analysis. Thus, 3659 daily maximum UHI values in the complete data set (all stations) were excluded from the analysis.

2.2. Data Analysis

[16] Our study focuses on determining the maximum UHI intensity during a diurnal cycle (UHI_{max}), and its statistical distribution, as well as on linking the UHI to greenness, surface water availability, and population density. To determine the UHI quantitatively, each urban station has been linked to meteorological observations at the closest KNMI rural station (Table 1 and Figure 1). Following the WMO instructions, the KNMI stations are located in well-vegetated and relatively flat terrain. Metainformation for these sites has been documented online at http://www.knmi.nl/klimatologie/metadata/. In principle, the choice for the closest KNMI station is straightforward, although some peculiarities may occur when the suggested reference station is located in different land surface conditions, e.g., stations close to the coast or to large lakes, or over a different soil type. In particular, the reference stations Wijk aan Zee and Zandvoort have been excluded as rural reference stations for the hobby stations in Leiden and Haarlem. Note that Valkenburg was taken as reference station for The Hague since both sites are located close to or within the dunes. Hence, taking into account the recommendation by *Sakakibara and Owa* [2005], Valkenburg acts as a natural reference for this station.

[17] In this study we define the UHI as the urban canyon air temperature minus the rural air temperature at screen level (2 m); it has been recorded on the basis of hourly data. However, the analysis focuses on the maximum UHI value in a diurnal cycle. Apart from climatological information, we also aim to quantify the differences between cities by quantifying the sensitivity of the recorded UHI to mean wind speed and daily integrated solar radiation S ($J\ cm^{-2}\ day^{-1}$). We hypothesize that UHI is related to the input of solar radiation, but at the same time we hypothesize different cities may absorb the radiation at a different efficiency as a result of difference in morphology or building material [*Oke*, 1982; *Mills*, 2009]. Hence, for each city we calculate $dUHI_{max}/dS$. In addition, physical intuition and earlier observations suggest that UHI will be inversely related to wind speed U. Calm

conditions inhibit heat transfer from the cities to the air layer aloft or to adjacent rural neighborhoods, which will enhance the UHI. To explore the differences among cites, we determine coefficient b in the following relation: $UHI_{max} \sim \exp(bU)$, with $b < 0$. Note, however, that *Conrads* [1975] found better agreement between the UHI and $\ln(U)$ than with U itself, although $\ln(U)$ will not behave physically for the limit case that $U \rightarrow 0$. Therefore, we prefer the exponential form proposed here.

2.3. Human Comfort

[18] For human beings, the experience of human comfort is in fact of more relevance than the UHI itself [*Budd* 2001, 2008]. Human comfort is governed by temperature, humidity, air movement, radiant temperature, clothing [*Havenith*, 1999], and metabolic rate [*Epstein and Moran*, 2006]. In addition, *Wang et al.* [2009] showed a direct correspondence between increased maximum and minimum temperature and the number of hospital admissions. In the current study, we will estimate the human comfort in urban neighborhoods by the wet bulb globe temperature (WBGT):

$$WBGT = 0.7T_w + 0.2T_g + 0.1T_a \quad (1)$$

Because the black globe temperature (T_g) is not a routinely observed variable, neither at the rural nor at the urban sites, we need to approximate the WBGT by

$$\mathrm{AWBGT} = 0.567T_a + 0.393e + 3.94, \quad (2)$$

where T_a is the air temperature and e is the water vapor pressure (hPa). Note that direct effects of wind and direct solar radiation are absent in this approximation. In addition, general AWBGT threshold values above which preventive action should be undertaken are not available, but they depend largely on a person's activities and clothing. For light work one should be careful for AWBGT > 30°C. For moderate and heavy work these thresholds are 26.7°C and 25°C, respectively (Sobane, 2011: Thermische omgevingsfactoren, Brussels, Belgium, available at http://www.ond.vlaanderen.be/welzijn/welzijnswetgeving/doc/algemeen/gezondheid/Brochure%20FOD%20Koude%20en%20Warmte.pdf). For the general public, an AWBGT < 27.7°C represents conditions without heat stress. For 27.7°C < AWBGT < 32.2°C the heat stress increases, and for AWBGT > 32.2°C great heat stress danger occurs. AWBGT > 31°C usually results in cancellation of public events. Physical training (e.g., sports) is not advised for AWBGT > 29.4°C.

[19] It is important to realize that other human comfort indicators have been derived in earlier studies, e.g., the particular mean vote [*Höppe*, 2002], physiological equivalent temperature, cooling power index, and discomfort index [*Kolokotsa et al.*, 2009]. However, many of these require knowledge of the human metabolism, which differs among groups and between individuals within such groups. As a result, these parameters, despite their physiologically solid grounding, cannot be determined as a general indicator of human comfort solely from meteorological information. Therefore, we limit ourselves to the AWBGT, although future studies should focus on confirming our findings using alternative variables.

2.4. Green and Water Cover Fraction

[20] This study examines whether the UHI and thermal comfort can be related to the morphological parameters of the selected cities. We aim to estimate the percentage of green and water cover in an area of 600 × 600 m around the observational site. This distance was found to represent the neighborhood scale reasonably well. With larger scales, the edges of the city and neighboring rural surroundings appeared in the analysis, overestimating the green urban cover. Conversely, with much shorter length scales (i.e., 50–100 m) green vegetation in the same neighborhood was not accounted for in the analysis. To estimate the green cover fraction, we utilize GoogleMaps™ images. To estimate the green vegetation cover, we use the fact that the reflection spectrum of green vegetation has a characteristic peak in the green band, while the reflection in the blue and red bands is substantially lower. At the same time, the reflectance in the blue band is substantially smaller than in the red band [*Sarlikioti et al.*, 2011]. Using these properties, we developed a new method to estimate the green and water cover of a city, as follows:

$$\%\mathrm{Green} = N^{-1} \sum_i x_{i|(R>1.2B)\wedge(G>1.01R)\wedge(G>1.01B)} \quad (3)$$

and

$$\%\mathrm{Water} = N^{-1} \sum_i x_{i|(B>1.06R)\wedge(B>1.01G)\wedge(G>R)\wedge(B>25)}. \quad (4)$$

Herein N is the number of pixels in the image, $x_i = 1$ if the conditions in the subscript are fulfilled, and $x_i = 0$ elsewhere. "Red," "green," and "blue" refer to the R, G and B values of the pixels.

[21] To ensure a skillful estimate of the green vegetation and water cover fraction by equations (3) and (4), its skill has been evaluated using a number of well-known land cover fractions. First, an image of a completely grass-covered region was selected, as well as an image of a fully water-covered region. From these images, a series of images with a variety of known green cover fractions was designed and consequently analyzed using equations (3) and (4).

[22] The validation of the designed method shows that the algorithm is well able to estimate the green cover fraction, though with a small bias of ~8%, though still with a high fraction of explained variance of 0.9998. For the water cover fraction, the bias is only ~2%, with and explained variance of 0.9999. Hence, we conclude that the developed algorithm is well suited for analyzing the green cover fraction and the water fraction for urban sites in the current research.

[23] Since the above method is based on properties of green, well-watered, and healthy vegetation, one should realize that our method likely performs best for satellite images taken in summer. Thus, the reported skill should be considered as an upper skill possible.

2.5. Extreme Value Statistics

[24] Usually UHI effects are recorded for short IOPs of a relatively limited number of days. Realizing that maximum UHI and AWBGT values are extreme values from a long series opens an alternative way of data analysis that has not, to

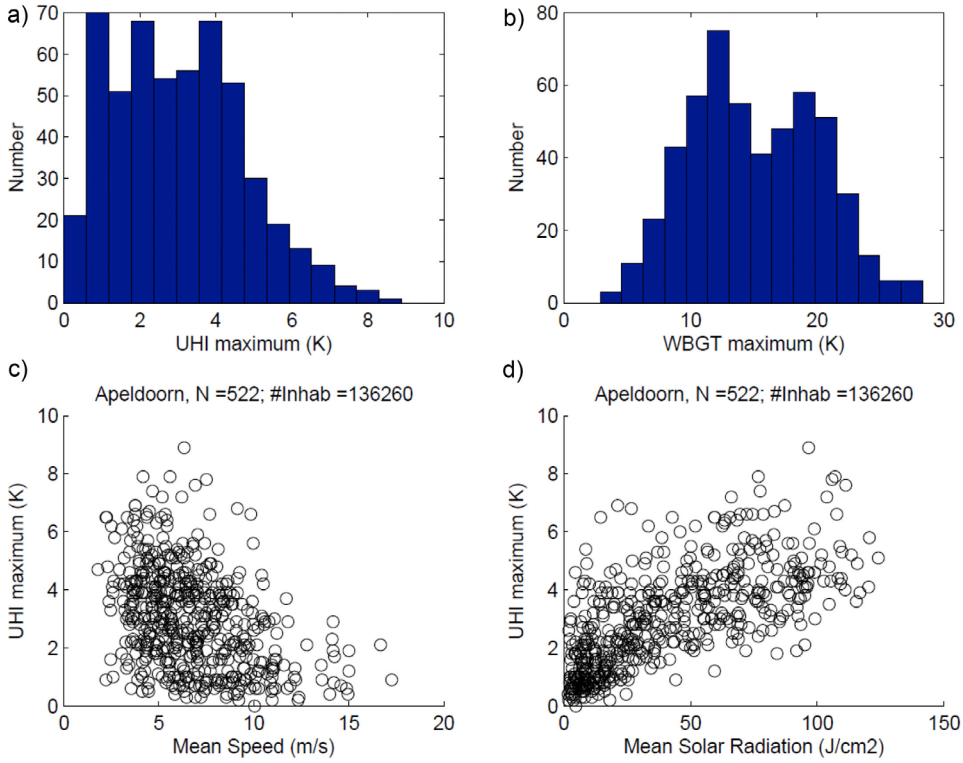

Figure 2. Distribution of the daily maximum of the (a) urban heat island effect (UHI) and (b) approximated wet bulb globe temperature (AWBGT) and sensitivity of the UHI to (c) wind speed and (d) solar radiation for Apeldoorn.

the authors' knowledge, been applied in urban weather and climate studies. To quantify the degree of extremity of the current observations, and to investigate whether these fit a statistical distribution for extreme value problems, we will fit our observations x (x being the maximum of the UHI or AWBGT) to the generalized extreme value (GEV) distribution ($F(x)$ is the cumulative distribution):

$$F(x) = \exp\left[-\left(1 - \frac{\kappa}{\alpha}(x-\mu)\right)^{1/\kappa}\right] \text{ for } \kappa \neq 0. \quad (5)$$

We will utilize the so-called L-moments approach to estimate the parameters κ, α and μ (see e.g., *Overeem et al.* [2008] for methodological details). Here, μ is middle value measure, κ is the shape parameter, and α is the scale parameter. L-moments are based on linear combinations of the order statistics of the daily maximum values of x. Since the L-moments method is not often used in urban meteorology, we briefly summarize the method in Appendix A. After obtaining the function $F(x)$ for each city, we can estimate the return time T of extreme values for variables of interest, $T = 1/(1 - F(x))$.

3. Basic Results

[25] First, we will discuss a number of interesting sites individually. As a first example we show the UHI distribution for Apeldoorn, which is a relatively small city but surrounded by natural vegetation, and as such not influenced by neighboring cities. It is also located ~150 km inland and is thus free of coastal influences. Apeldoorn experiences a skewed UHI distribution, with a median of 2.8 K and a 95 percentile of 6.0 K (Figure 2a). Figures 2b and 2c show a typical dependence of UHI on its main atmospheric forcings, namely that UHI is approximately linear in the received solar radiation and inverse proportional to the wind speed. For Apeldoorn, $dUHI_{max}/dS \cong 0.037$ K/W m^{-2}, and coefficient $b \cong -0.69$ s m^{-1}. It is interesting to compare $dUHI_{max}/dS$, and coefficient b as reported for Apeldoorn with results from other cities. Averaged over all cities, $dUHI_{max}/dS$ was 0.028 K/W m^{-2}, with an interquantile range of 0.024 K/W m^{-2} and a coefficient of variation of 0.66. For b, a mean value of −0.61 s m^{-1} was found, with an interquantile range of 0.18 s m^{-1} and a coefficient of variation of −0.31. Hence it appears that the relative contribution of solar radiation to the UHI differs more between cities than it does for wind speed. From Figure 2b, it is suggested that the AWBGT has a bimodal distribution, and the threshold of 27.7°C is not exceeded in Apeldoorn. However, this bimodal distribution has not been found for most of the other sites. The bimodal distribution for Apeldoorn is likely caused by the individual effects of temperature and humidity that do not always coincide. In certain summer regimes, enhanced solar radiation will lead to increased surface temperature and consequently enhanced convective turbulence. As a consequence, dry air entrainment will reduce the boundary layer humidity, and, hence, the increased temperature does not coincide with increased humidity, giving a possible reason for the bimodal distribution. This hypothesis is, however, open for further evaluation from observational and modeling perspective.

[26] The results for Rotterdam are of particular interest. Despite its location close to the coast and its high water availability in the harbors, the UHI is particularly large, with a

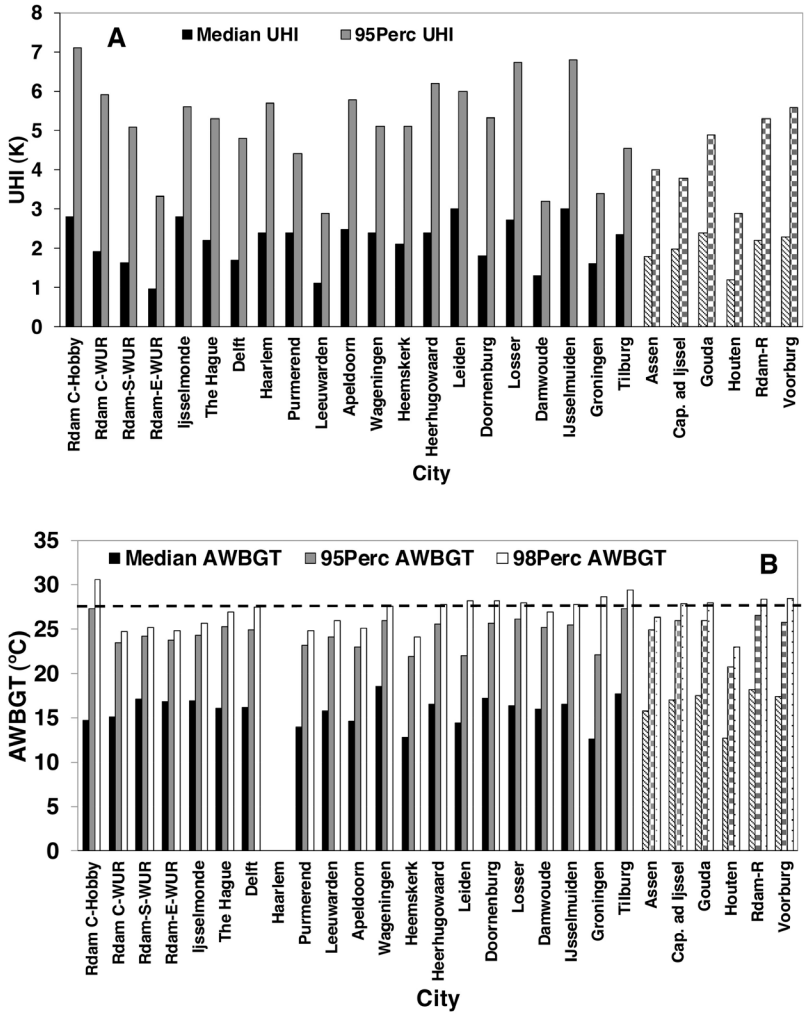

Figure 3. Observed median and percentile values of the (a) canopy layer UHI and (b) AWBGT for the studied cities in the Netherlands. The roof-level stations are shown in modified fill.

median and 95 percentile of 2.8 K and 7.2 K, respectively. From Figure 3, we find that Rotterdam experiences a substantial heterogeneity of the UHI. The WUR weather stations show a smaller UHI compared to the hobby meteorological station, although we should keep in mind that the statistics for the two stations are not based on the same observational period, and thus the intercomparison should be considered preliminary. Also, the WUR center station is located on a balcony close to the building roof, while the hobby station was installed on a roof. However, the differences among the WUR stations are based on the same observational episode, and they show a ranking with a high UHI in the city center and smaller values in the southern and eastern stations further away from the center. The median UHI for the eastern station is ~2.5 K smaller than for the city center, while the 95 percentile is even ~3 K smaller than for the city center. Hence, substantial UHI differences occur within Rotterdam, as has been confirmed by a number traverse measurements documented by *Heusinkveld et al.* [2010].

[27] Furthermore, it is worth noting that even a relatively small city such as Losser is subject to relatively high values of the UHI and also to heat stress (see below). However, this city is located far inland and experiences a land climate. Conversely, we find small UHI effects, compared to other cities, in Groningen, Assen, Damwoude, and Leeuwarden. These cities are all located in the north of the country and relatively close to the coast, and they report on average a higher wind speed compared to the rest of the country. As seen in Figure 2c, the higher wind speed is highly likely responsible for the smaller UHI. To summarize, for all cities the mean value and 95 percentile of the daily maximum UHI are 2.3 K and 5.3 K, respectively. However, the difference between locations can be relatively large.

[28] We repeated our analysis using an alternative definition for UHI, namely, the difference between the minimum temperature in the city and in the rural surroundings, UHI_{TMIN}. This definition is sometimes used in modeling studies [e.g., *McCarthy et al.*, 2010], and therefore it is interesting to study the sensitivity of the results to the UHI definition. UHI_{TMIN} was found to be on average only 0.6 K and the 95 percentile of UHI_{TMIN} was 3.2 K, which is substantially lower than UHI based on hourly observations. On average, the UHI was about 1.7 K and 2.0 K smaller for the median and 95 percentile UHI, respectively, in the case where

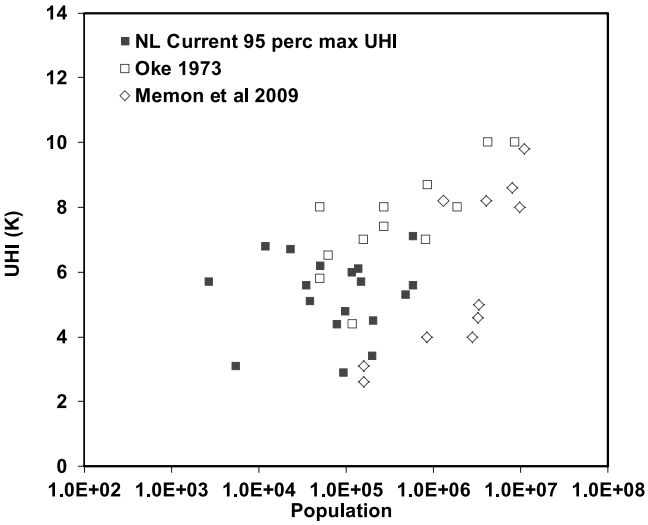

Figure 4. UHI for Dutch cities (urban canopy layer observations only) in the current study (filled symbols) and for other European cities (open symbols).

UHI_{TMIN} was used as criterion. Hence, hourly observations are recommended for detection of the daily maximum UHI (see also *Stewart* [2011]).

[29] The current results for the Netherlands can be compared with model and observational results for the canopy layer urban heat island for other cities in Europe (Figure 4), though differences in experimental approaches should be kept in mind. *Johnson* [1985] found a mean UHI_{max} of 4.7 K for Birmingham, while *Eliasson* [1996] reports a mean UHI of 4 K for Göteborg. *Oke* [1973] reviewed the UHI for European cities and found $5.7 < UHI_{max} < 10.0$ K, and for the only Dutch city in the review, Utrecht, UHI ~ 6 K was reported. More recently, the UHI for Toulouse was found to be 5 K [*Hidalgo et al.*, 2008]. Figure 4 compares UHI as documented by *Oke* [1973] and *Memon et al.* [2009] with the current results. It is evident that the spread in the current observations is larger than in the simple and intuitive relation between population and UHI_{max} presented by *Oke* [1973]. This observation suggests that the UHI_{max} in the Netherlands is determined by variables or parameters other than city population, e.g., sky view factor, vegetation cover, and water surface cover, as found in earlier studies.

[30] Figure 5 shows the relation between the median and the 95 percentile of the daily maximum UHI. There is a clear relation between the median and the 95 percentile. Consequently, for cities for which the mean UHI is known, the extreme value can be estimated using this seemingly robust relation.

[31] In addition to the UHI, cities also experience a so-called shadow effect or cool island effect. Buildings at the edge of a city inhibit penetration of sunlight into the city canyon during the first hours after sunrise. As a result, during the early morning hours, cities can be colder than the rural surroundings [*Oke*, 1982]. In the current study, all cities in the Netherlands appear to experience this shadow effect. The average cool island effect amounts to −1.2 K, while we found the largest cooling island in Heemskerk, −1.9 K, and the smallest in Rijnmond, −0.1 K. The latter is consistent with the fact that the instrument in Rijnmond was located at 30 m above the ground, and shadowing effects are limited. This physically consistent picture confirms that the hobby meteorological stations in general reflect meaningful observations.

[32] Finally, since the dependence of UHI on its forcings appears rather robust among the cities, we may deduce additional confidence in the hobby meteorological observations.

4. Heat Stress Relation

4.1. Median Values

[33] Concerning the heat stress, we find relatively low median values for the AWBGT for all cities (Figure 3b), all far below the threshold value of 27.7°C. However, the 95 and 98 percentile for the cities are close to the threshold values mentioned earlier. Rotterdam reports a 95 percentile of 27.3°C, which is close to the threshold value of 27.7°C. Its 98 percentile is even 30.6°C, substantially above the suggested threshold value. This means that on 4.1% of the days, the AWBGT exceeds 27.7°C, i.e., ~15 days per year. On 0.5% of the days, the AWBGT exceeds 32.2°C, i.e., 2 days per year. The data series is, however, too short to allow the very high percentiles to be estimated robustly. Overall, in 7 of the 20 cities, the threshold for onset of heat stress is exceeded for the 98 percentile. In other words, 35% of the cities under investigation experience heat stress for 7 days a year.

[34] Considering the heterogeneity of the AWBGT in the city of Rotterdam, we find relative small differences in heat stress, with slightly higher values for the southern and eastern stations. Since both showed lower temperatures compared to the city center, the higher AWBGT must be due to higher specific humidity in the city outskirts. This observation is consistent with the higher availability of evaporating vegetation in the outskirts.

[35] It is should be noted that this study covers only single-day heat doses as represented by AWBGT. However, it will be interesting for future studies to document the effect of multiday exposure to high AWBGT on human comfort.

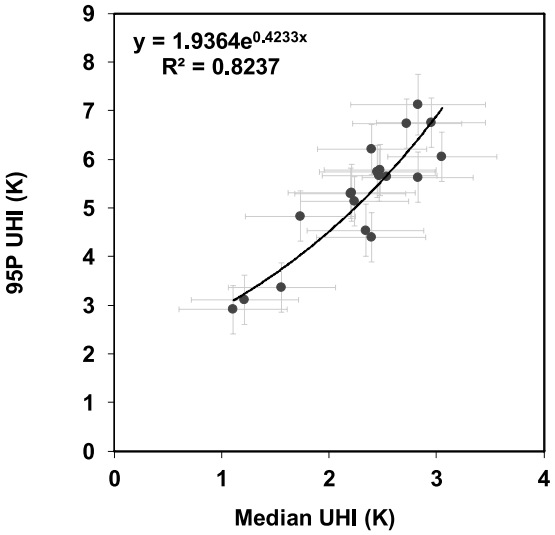

Figure 5. Relation between 95 percentile of the daily maximum UHI and the median of the maximum daily UHI. Note: only observations from the urban canopy layer have been used.

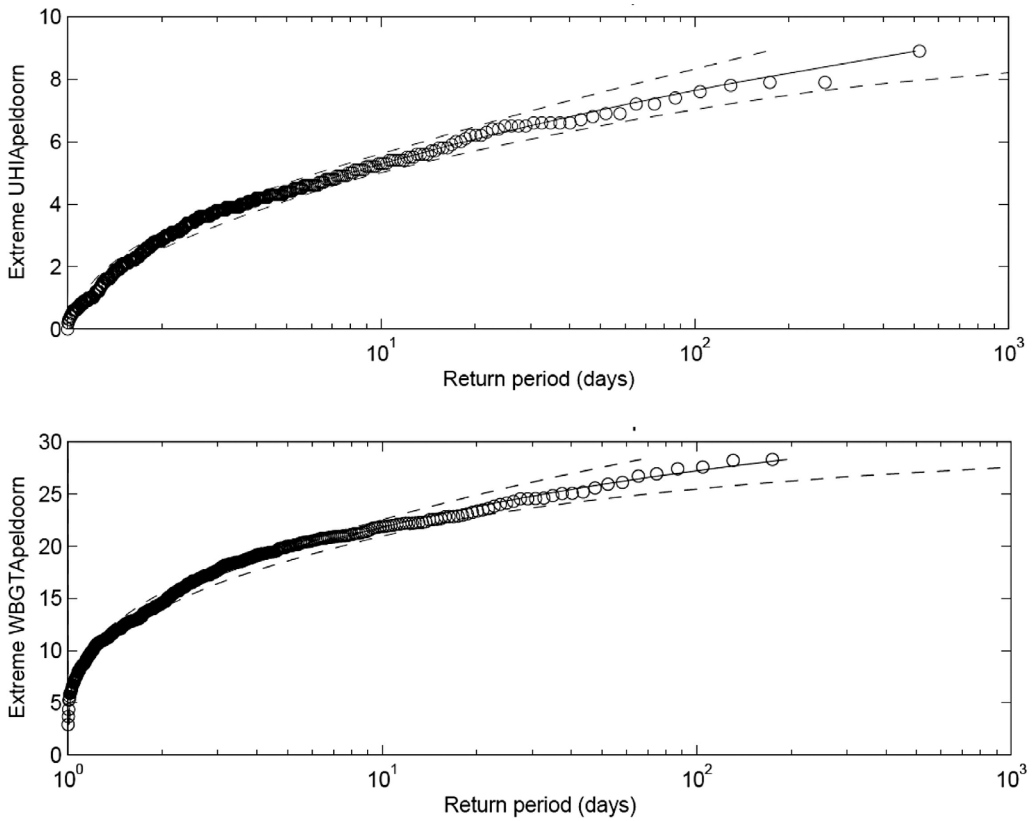

Figure 6. Observed daily maximum UHI versus the observed return period for the city of Apeldoorn. The reduced variable is $-\ln\{-\ln[n/(n_{tot}+1)]\}$, with n being the nth ranked observation and n_{tot} being the total number of observations. The solid line indicates the fit to the generalized extreme value (GEV) distribution, and the dashed lines give the upper and lower boundary obtained from the bootstrapping.

4.2. Extreme Value Statistics

[36] Figure 6 shows that the UHI and AWBGT observations for Apeldoorn follow the proposed GEV distribution rather well, and this trend has been confirmed for most of the other observational stations. Thus, the GEV seems a useful tool for UHI analysis. For Apeldoorn, a daily maximum UHI effect of 5 K appears to have a return period of approximately 7 days, while the return period is about 140 days for UHI = 8 K. A substantial difference has been found for the GEV parameters for different cities (Table 3). The average return time for a daily maximum UHI of 5 K over the cities studied in this paper appears to be 41 days, although the median is 14 days. This discrepancy indicates substantial differences between cities. For the AWBGT threshold value of 27.7 K, a mean and median return period of 79 and 44 days, respectively, was found. Note, however, that for summer days this return period will be much smaller than reported here. However, the current data set does not cover a sufficient number of summer days to allow robust estimation of return periods by season. Hence, we limit ourselves to comparing cities on the basis of full year-round observations.

[37] To estimate the uncertainty of the achieved return periods of heat stress events in terms of UHI or AWBGT, we use the bootstrapping statistical method. The bootstrapping method is based on a resampling (with redrawing) within the original data set (in this case for $AWBGT_{max}$) and reestima-

Table 3. Parameters GEV for UHI and AWBGT Distribution

	UHI			AWBGT		
	μ	κ	α	μ	κ	α
Urban Canyon Stations						
Rotterdam	2.199	−0.068	1.544	13.363	0.004	4.767
The Hague	1.740	0.013	1.326	14.775	0.238	5.459
Delft	1.244	0.008	1.181	14.438	0.265	5.476
Haarlem	1.926	0.085	1.363			
Purmerend	2.080	0.175	1.033	12.873	0.143	4.614
Leeuwarden	0.869	−0.094	0.617	14.068	0.241	5.068
Apeldoorn	2.147	0.113	1.554	13.137	0.225	4.928
Wageningen	1.783	0.116	1.344	16.398	0.420	5.778
Heemskerk	1.709	0.037	1.226	11.101	0.148	4.585
Heerhugowaard	1.784	−0.011	1.528	14.667	0.222	5.222
Leiden	2.505	0.081	1.348	12.378	0.210	4.587
Doornenburg	3.192	0.173	1.846	14.983	0.287	5.796
Losser	2.080	−0.011	1.583	14.195	0.239	5.650
Damwoude	0.989	−0.028	0.687	14.130	0.249	5.395
IJsselmuiden	2.303	0.055	1.669	14.450	0.248	5.524
Groningen	1.243	0.033	0.831	10.697	0.149	4.894
IJsselmonde	2.270	0.096	1.384	15.095	0.332	5.058
Tilburg	1.727	0.133	1.294	15.470	0.369	6.801
Roof Stations						
Houten	0.820	0.092	0.858	11.366	0.199	4.430
Voorburg	1.719	0.034	1.519	15.550	0.263	5.249
Assen	1.460	−0.078	0.896	14.060	0.234	5.263
Gouda	1.912	0.072	1.148	15.672	0.267	5.078
Rijnmond	1.614	0.069	1.373	15.879	0.339	5.732
Capelle a/d IJssel	1.537	0.219	1.091	14.848	0.313	5.868

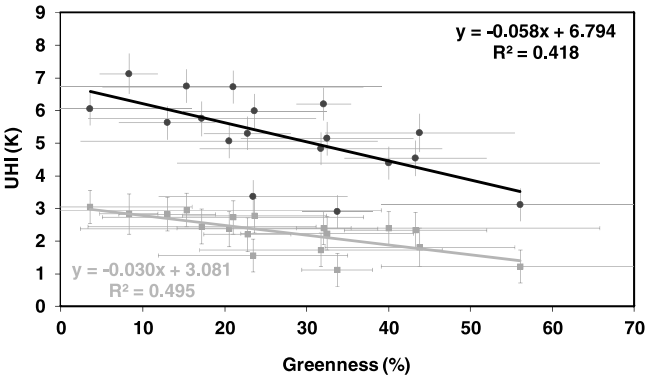

Figure 7. Observed median (gray) and 95 percentile (black) of maximum daily UHI as function of fraction of green cover. Note: only observations from the urban canopy layer have been used.

tion of the parameters in the GEV distribution, using the same method as for the original data set. In the current study, we have chosen to determine the uncertainty by using 1000 bootstrap samples. It is evident that the uncertainty of the return period increased substantially for larger UHI. For Apeldoorn, the uncertainty is only 1 day for low return periods, while for the larger UHI it is roughly tens of days. Considering the extreme values of the AWBGT, the return period for the mentioned threshold of 27.7°C approaches approximately ~110 days, through the uncertainty is rather large, since the confidence interval ranges from 70 to $\sim 10^3$ days. Finally, we wish to mention that for a number of stations, the return times for AWBGT and UHI are not always very consistent. For Houten, Leiden, Heemskerk, Apeldoorn, and IJsselmonde, the return period for AWBGT is much larger than for UHI.

[38] It is valuable to remark here that a large effort has been undertaken in the development and evaluation of land surface schemes for the urban environment [*Kusaka et al.*, 2001; *Masson*, 2000; *Martilli*, 2007; *Grimmond et al.*, 2010, 2011]. The evaluation of these schemes focuses particularly on the representation of turbulent surface fluxes and heat storage in buildings. However, some schemes [e.g., *Kusaka et al.*, 2001] do forecast the 2 m temperature in the city. It is tempting to also evaluate whether these schemes reproduce a similar shape of UHI_{max}, and whether these follow the GEV distribution as well. This alternative methodology for a future study may provide evaluation on a different scale and is therefore of added value.

5. Urban Heat Island Effects

5.1. Relation to Urban Morphology and Topology

[39] In terms of urban planning, it is interesting to discuss the role of urban green vegetation cover on UHI and human comfort. Table 1 indicates that among Dutch cities the extent of green vegetation and water cover varies widely. In particular, the water bodies and canals in Rotterdam, Leiden, and Delft are responsible for the high percentage of water cover. For IJsselmuiden, the large water cover is due to the river IJssel being close by at the western part of the site. Greenness is widely variable among the cities as well. The relatively low green cover in Rotterdam, Wageningen, and Leiden is due to the densely built up area in the neighborhood of the weather station.

[40] From Figure 7, which shows the UHI for the stations located in the canyons as a function the urban green cover, we find an evident relation between the green vegetation cover and both the median and 95 percentile of the maximum daily UHI values. Despite the substantial uncertainties in the analysis performed, in both cases UHI decreases with urban green cover, though the magnitude of the slope is larger for the 95 percentile than for the median UHI. This trend suggests that urban green vegetation has the largest impact on the extremely hot days and also confirms the hypothesis that green vegetation cover is a possibly effective measure to mitigate strong urban heat islands. A two-tailed Student's t test confirms the significance of this relation with $p < 0.0011$ for the constant in both linear regressions, and $p = 0.004$ and $p = 0.016$ for the slopes of the median and 95 percentile, respectively. Note, however, that for both regressions, the limit behavior for large green cover fractions is not correct, since a value for green vegetation cover of 100% does not result in vanishing UHI values. This result is likely due to lack of data in this range of the green cover fraction, as well to as other variables that will govern UHI. We underline that including data from the roof level resulted in a substantial deterioration of the relation between UHI and green vegetation cover, i.e., R^2 decreased from 0.38 to 0.23 for the 95 percentiles and from 0.44 to 0.32 for the median, when roof stations were included. This result further illustrates that hobby meteorological data should be studied with care and with a conceptual framework in mind.

[41] Furthermore, it is interesting to note that we did not find a solid relation between UHI and water cover fraction (not shown). The low thermal inertia of water bodies could be a possible explanation for this effect. Though water temperature responds slowly to forcing during the day, it also cools down slowly, which means that large water bodies support the urban heat island effect at night.

[42] Since UHI appears to be closely related to the urban green vegetation cover, a corresponding relation could be hypothesized for human comfort, or AWBGT. However, such a relation does not appear from our current analysis. This result is possibly due to the enhanced specific humidity resulting from evapotranspiration by the vegetation.

5.2. Relation to Population Density

[43] Finally, we report on the relation between the observed UHI and aspects of population density. For this part of the study, the population density was extracted from the national institute for statistics [*Centraal Bureau voor de Statistiek* (CBS), 2009]. Their classification of neighborhoods is based on differences in landscapes or socioeconomic structure, and within urban units the classification is as much as possible based on uniformity of the building design. Classification of units with scattered building structure is based on local insights about land use and dominance of certain architecture. Note that the CBS classification does not a priori match the scale of the assessment of water and vegetation cover in section 4.

[44] From our study, it appears that total city population is not well correlated with UHI. However, we can hypothesize that UHI is better correlated with population density of the neighborhood since higher population density requires higher

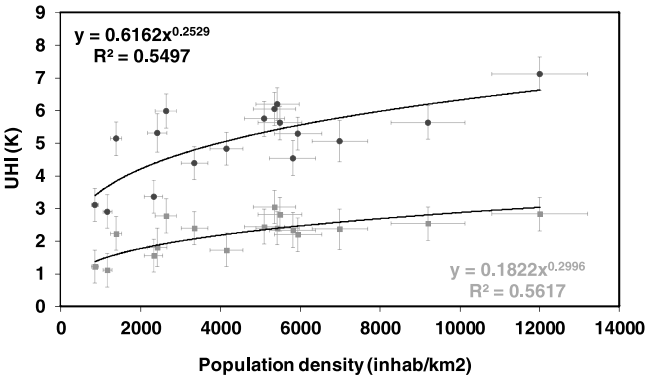

Figure 8. Observed median (gray) and 95 percentile (black) of the daily maximum UHI effect for Dutch cities versus population density at neighborhood scale. Note that only observations from the urban canopy layer have been used.

building density and, hence, results in enhanced radiation trapping and high thermal inertia. Anthropogenic emissions will be enhanced as well. Figure 8 shows that both the median and the 95 percentile increase with population density, although scatter is particularly large for the 95 percentile. Note, the reader should be careful in interpreting the right tail of the graphs, because only one site was available with a population density of more than 8000 inhabitants per square kilometer. For both quantities, we find approximately a 1/4-power relation. The finding that UHI is better correlated with population density than with population confirms earlier findings from *Oke* [1982] and at the same time support our confidence in the gathered observations.

6. Final Remarks

[45] In this paper, we use the AWBGT as a measure for human comfort. However, it is important to note that the practical use of this approach to account for heat stress is limited in cities, since the AWBGT is based on a steady state model and may not a priori represent the sensation of heat. In addition, because of the heterogeneous nature of cities, people experience continuously different radiation and wind conditions, so a steady state will hardly ever be reached. On the other hand, outcomes of steady state models correlate well with increased mortality due to heat [*Höppe*, 2002], and thus the tool is suited to our research aim.

[46] Furthermore, it is important to recognize that from a physiological point of view the AWBGT is perhaps not the most suitable measure for heat stress. The most serious limitation of AWBGT is that it does not adequately reflect the additional strain people experience when the evaporation of sweat is restricted by high humidity or low air movement. However, *Budd* [2008] remarks that indicators that are not ideal from the physiological perspective are still suitable as a general guide for human comfort, e.g., for longer term climatic studies as reported in this paper.

7. Conclusions

[47] This paper quantifies the magnitude of the urban canyon layer heat island effect UHI and a human comfort index in the Netherlands. Furthermore, we studied the relation between UHI and neighborhood population density and green cover fraction. Because official observations are lacking, our novel analysis is based on high-quality observations by hobby meteorologists. The average maximum UHI during a diurnal cycle is 2.3 K, while the average 95 percentile over all cities is 5.3 K. Furthermore, observational sites above the canyon layer show a different behavior than those within the canyon layer. The statistical distribution of the human comfort expressed in the approximated wet bulb globe temperature (AWBGT) shows a bimodal distribution for some cities. It is found that approximately 50% of the urban areas in this research are subject to heat stress for about 7 days per year. In particular, the city of Rotterdam exceeds the heat stress threshold value for about 15 days per year.

[48] Also, it appears that most of the daily maximum observations, for both UHI and human comfort, follow a GEV distribution closely, and the return periods for heat stress can be determined. Also, we quantify the uncertainty in this return period by applying a bootstrapping method. These uncertainties are relatively small for return periods smaller than 100 days but become substantially larger for longer return periods, indicating that the current data series is relatively short for detecting the tails of the GEV distribution with great confidence.

[49] Finally, our study shows that UHI is more correlated with population density at neighborhood scale than to the number of total inhabitants in the city. Also, a significant negative correlation between green cover fraction and both the media UHI and the 95 percentile of the UHI was established. However, a network of observations within the Rotterdam metropolis indicates substantial differences in the canyon layer UHI within a city.

Appendix A: L Moments Method

[50] As a first step, the probability-weighted moments based on n samples are estimated by

$$b_0 = n^{-1}\sum_{j=1}^{n} x_j, \tag{A1}$$

$$b_1 = n^{-1}\sum_{j=2}^{n} \frac{j-1}{n-1} x_j, \tag{A2}$$

$$b_2 = n^{-1}\sum_{j=3}^{n} \frac{(j-1)(j-2)}{(n-1)(n-2)} x_j, \tag{A3}$$

where x_j are the ordered samples of the daily maxima. Subsequently, the sample L moments are then obtained as

$$l_1 = b_0, \tag{A4}$$

$$l_2 = 2b_1 - b_0, \tag{A5}$$

$$l_3 = 6b_2 - 6b_1 + b_0. \tag{A6}$$

The estimate of the shape parameter κ follows from

$$\hat{\kappa} = 7.8590c + 2.9954c^2, \tag{A7}$$

where

$$c = \frac{2}{3 + l_3/l_2} - \frac{\ln(2)}{\ln(3)}. \quad \text{(A8)}$$

The estimates of α and μ are subsequently obtained as

$$\hat{\alpha} = \frac{l_2 \hat{\kappa}}{(1 - 2^{-\hat{\kappa}})\Gamma(1 + \hat{\kappa})}, \quad \text{(A9)}$$

and, using the gamma function $\Gamma(x)$,

$$\hat{\mu} = l_1 - \hat{\alpha} \frac{1 - \Gamma(1 + \hat{\kappa})}{\hat{\kappa}}. \quad \text{(A10)}$$

[51] **Acknowledgments.** The authors acknowledge the hobby meteorologists who provided observations that made this study possible: K. Piening, H. Beek, S. Rosdorff, M. van der Hoeven, M. van der Molen, M. de Kleer, M. Borgardijn, S. Roelvink, W. ter Haar, F. Bijlsma, R. Zwolsman, R. Khoe, J. Kruijsen, O. de Zwart, J. Effing, W. van Dijk, M. Peters, M. van Maanen, W. van der Velde, J. Spruijt, H. Lankamp, H. van der Heide, G. van 't Klooster, C. Pel, M. Gosselink, F. Brouwer, W. van Duijn. Also, we acknowledge Jan Elbers (Wageningen UR) for setting up and maintaining the WUR weather stations in Rotterdam. Furthermore, we thank the Royal Netherlands Meteorological Institute for providing the observations for rural areas. In addition, the authors acknowledge financial support from Climate Changes Spatial Planning and the Knowledge for Climate research programs. We are grateful to GoogleMaps™ for making available spatial information from aerial photography, as well as the Dutch digital elevation model (Actueel Hoogtebestand Nederland, http://www.ahn.nl/). Finally we are grateful to three anonymous reviewers for their valuable comments and suggestions.

References

Ali-Toudert, F. A., and H. Mayer (2006), Numerical study on the effects of aspect ratio and orientation of an urban street canyon on outdoor thermal comfort in hot and dry climate, *Build. Environ.*, *41*, 94–108, doi:10.1016/j.buildenv.2005.01.013.

Budd, G. M. (2001), Assessment of thermal stress—The essentials, *J. Therm. Biol.*, *26*, 371–374, doi:10.1016/S0306-4565(01)00046-8.

Budd, G. M. (2008), Wet-bulb globe temperature (WBGT)—Its history and its limitations, *J. Sci. Med. Sport*, *11*, 20–32, doi:10.1016/j.jsams.2007.07.003.

Centraal Bureau voor de Statistiek (CBS) (2009), Buurtkaart met cijfers 2008, 9 pp., The Hague, Netherlands.

Conrads, L. A. (1975), Observations of meteorological urban effects. The heat island of Utrecht, Ph.D. thesis, 83 pp., Univ. of Utrecht, Utrecht, Netherlands.

Coutts, A. M., J. Beringer, and N. J. Tapper (2008), Investigating the climatic impact of urban planning strategies through the use of regional climate modelling: A case study for Melbourne, Australia, *Int. J. Climatol.*, *28*, 1943–1957, doi:10.1002/joc.1680.

Dandou, A., M. Tombrou, E. Akylas, N. Soulakellis, and E. Bossioli (2005), Development and evaluation of an urban parameterization scheme in the Penn State/NCAR Mesoscale Model (MM5), *J. Geophys. Res.*, *110*, D10102, doi:10.1029/2004JD005192.

Dieleman, F. M., M. J. Dijst, and G. Burghouwt (2002), Urban form and travel behavior: Micro-level household attributes and residential context, *Urban Stud.*, *39*, 507–527, doi:10.1080/00420980220112801.

Dimoudi, A., and M. Nikolopoulou (2003), Vegetation in the urban environment: Microclimate analysis and benefits, *Energy Build.*, *35*, 69–76, doi:10.1016/S0378-7788(02)00081-6.

Eliasson, I. (1996), Urban nocturnal temperatures, street geometry and land use, *Atmos. Environ.*, *30*, 379–392, doi:10.1016/1352-2310(95)00033-X.

Epstein, Y., and D. S. Moran (2006), Thermal comfort and the heat stress indices, *Ind. Health*, *44*, 388–398, doi:10.2486/indhealth.44.388.

Floor, C. (1970), Onderzoek Utrechts stadsklimaat met weerbus, *Hemel Dampkring*, *68*, 107–111.

Godowitch, J. M., J. K. S. Ching, and J. F. Clarke (1985), Evolution of the nocturnal inversion layer at an urban and nonurban site, *J. Clim. Appl. Meteorol.*, *24*, 791–804, doi:10.1175/1520-0450(1985)024<0791:EOTNIL>2.0.CO;2.

Grimmond, C. S. B., et al. (2010), The International Urban Energy Balance Models Comparison Project: First results from phase 1, *J. Appl. Meteorol. Climatol.*, *49*, 1268–1292, doi:10.1175/2010JAMC2354.1.

Grimmond, C. S. B., et al. (2011), Initial results from phase 2 of the international urban energy balance comparison project, *Int. J. Climatol.*, *31*, 244–272, doi:10.1002/joc.2227.

Havenith, G. (1999), Heat balance when wearing protective clothing, *Ann. Occup. Hyg.*, *43*, 289–296, doi:10.1093/annhyg/43.5.289.

Heusinkveld, B. G., L. W. A. van Hove, C. M. J. Jacobs, G. J. Steeneveld, J. A. Elbers, E. J. Moors, and A. A. M. Holtslag (2010), Use of a mobile platform for assessing urban heat stress in Rotterdam, in *Proceedings of the 7th Conference on Biometeorology Albert-Ludwigs-University of Freiburg, Germany, 12-14 April 2010*, *Ber. 20*, pp. 433–438, Meteorol. Inst., Univ. Freiburg, Freiburg, Germany.

Hidalgo, J., G. Pigeon, and V. Masson (2008), Urban-breeze circulation during the CAPITOUL experiment: Experimental data analysis approach, *Meteorol. Atmos. Phys.*, *102*, 223–241, doi:10.1007/s00703-008-0329-0.

Hinkel, K. M., and F. E. Nelson (2007), Anthropogenic heat island at Barrow, Alaska, during winter: 2001–2005, *J. Geophys. Res.*, *112*, D06118, doi:10.1029/2006JD007837.

Höppe, P. (2002), Different aspects of assessing indoor and outdoor thermal comfort, *Energy Build.*, *34*, 661–665, doi:10.1016/S0378-7788(02)00017-8.

Johnson, D. B. (1985), Urban modification of diurnal temperature cycles in Birmingham, U.K., *J. Climatol.*, *5*, 221–225, doi:10.1002/joc.3370050208.

Kanda, M. (2007), Progress in urban meteorology, *J. Meterol. Soc. Jpn.*, *85B*, 363–383, doi:10.2151/jmsj.85B.363.

Kolokotsa, D., A. Psomas, and E. Karapidais (2009), Urban heat island in southern Europe: The case study of Hania, Crete, *Sol. Energy*, *83*, 1871–1883, doi:10.1016/j.solener.2009.06.018.

Köppen, W. (1931), *Klimakarte der Erde*, 2nd ed., Grundriss der Klimakunde, Berlin.

Krpo, A., F. Salamanca, A. Martilli, and A. Clappier (2010), On the impact of anthropogenic heat fluxes on the urban boundary layer: A two-dimensional numerical study, *Boundary Layer Meteorol.*, *136*, 105–127, doi:10.1007/s10546-010-9491-2.

Kusaka, H., H. Kondo, Y. Kikegawa, and F. Kimura (2001), A simple single-layer urban canopy model for atmospheric models: Comparison with multi-layer and slab models, *Boundary Layer Meteorol.*, *101*, 329–358, doi:10.1023/A:1019207923078.

Lenzuni, P., D. Freda, and M. Del Gaudio (2009), Classification of thermal environments for comfort assessment, *Ann. Occup. Hyg.*, *53*, 325–332, doi:10.1093/annhyg/mep012.

Martilli, A. (2007), Current research and future challenges in urban mesoscale modeling, *Int. J. Climatol.*, *27*, 1909–1918, doi:10.1002/joc.1620.

Masson, V. (2000), A physically based scheme for the urban energy budget in atmospheric models, *Boundary Layer Meteorol.*, *94*, 357–397, doi:10.1023/A:1002463829265.

McCarthy, M. P., M. J. Best, and R. A. Betts (2010), Climate change in cities due to global warming and urban effects, *Geophys. Res. Lett.*, *37*, L09705, doi:10.1029/2010GL042845.

Memon, R. A., D. Y. C. Leung, and C.-H. Liu (2009), An investigation of urban heat island intensity (UHII) as an indicator of urban heating, *Atmos. Res.*, *94*, 491–500, doi:10.1016/j.atmosres.2009.07.006.

Mills, G. (2009), Micro- and mesoclimatology, *Prog. Phys. Geogr.*, *33*, 711–717, doi:10.1177/0309133309345933.

Mimet, A., V. Pellissier, H. Quénol, R. Aguejdad, V. Dubreuil, and F. Rozé (2009), Urbanisation induces early flowering: Evidence from *Platanus acerifolia* and *Prunus cerasus*, *Int. J. Biometeorol.*, *53*, 287–298, doi:10.1007/s00484-009-0214-7.

Oke, T. R. (1973), City size and the urban heat island, *Atmos. Environ.*, *7*, 769–779, doi:10.1016/0004-6981(73)90140-6.

Oke, T. R. (1976), The distinction between canopy and boundary-layer urban heat islands, *Atmosphere*, *14*, 269–277, doi:10.1080/00046973.1976.9648422.

Oke, T. R. (1982), The energetic basis of the urban heat island, *Q. J. R. Meteorol. Soc.*, *108*, 1–24, doi:10.1002/qj.49710845502.

Oke, T. R. (2006), Initial guidance to obtain representative meteorological observations at urban sites, *IOM Rep. 81*, World Meteorol. Org., Geneva.

Overeem, A., A. Buishand, and I. Holleman (2008), Rainfall depth-duration-frequency curves and their uncertainties, *J. Hydrol.*, *348*, 124–134, doi:10.1016/j.jhydrol.2007.09.044.

Reid, C. E., M. S. O'Neill, C. J. Gronlund, S. J. Brines, D. G. Brown, A. V. Diez-Roux, and J. Schwartz (2009), Mapping community determinants of heat vulnerability, *Environ. Health Perspect.*, *117*, 1730–1736, doi:10.1289/ehp.0900683.

Runnalls, K. E., and T. R. Oke (2000), Dynamics and controls of the near-surface heat island of Vancouver, B.C., *Phys. Geogr.*, *21*, 283–304.

Sakakibara, Y., and K. Owa (2005), Urban-rural temperature differences in coastal cities: Influence of rural sites, *Int. J. Climatol.*, *25*, 811–820, doi:10.1002/joc.1180.

Sarlikioti, V., E. Meinen, and L. F. M. Marcelis (2011), Crop reflectance as a tool for the online monitoring of LAI and PAR interception in two different greenhouse crops, *Biosys. Eng.*, *108*, 114–120, doi:10.1016/j.biosystemseng.2010.11.004.

Souch, C., and S. Grimmond (2006), Applied climatology: Urban climate, *Prog. Phys. Geogr.*, *30*, 270–279, doi:10.1191/0309133306pp484pr.

Stewart, I. D. (2011), A systematic review and scientific critique of methodology in modern urban heat island literature, *Int. J. Climatol.*, *31*, 200–217, doi:10.1002/joc.2141.

Stewart, I. D., and T. R. Oke (2010), Thermal differentiation of local climate zones using temperature observations from urban and rural field sites, paper presented at the Ninth Symposium on Urban Environment, Am. Meteorol. Soc., Keystone, Colo., 2–6 Aug.

Svensson, M. K. (2004), Sky view factor analysis-implications for urban air temperature differences, *Meteorol. Appl.*, *11*, 201–211, doi:10.1017/S1350482704001288.

Svensson, M. K., and I. Eliasson (2002), Diurnal air temperatures in built-up areas in relation to urban planning, *Landscape Urban Plann.*, *61*, 37–54, doi:10.1016/S0169-2046(02)00076-2.

Synnefa, A., A. Dandou, M. Santamouris, M. Tombrou, and N. Soulakellis (2008), On the use of cool materials as a heat island mitigation strategy, *J. Appl. Meteorol. Climatol.*, *47*, 2846–2856, doi:10.1175/2008JAMC1830.1.

Takebayashi, H., and M. Moriyama (2009), Study on the urban heat island mitigation effect achieved by converting to grass-covered parking, *Sol. Energy*, *83*, 1211–1223, doi:10.1016/j.solener.2009.01.019.

United Nations (2005), World urbanization prospects: The 2005 revision, Dep. of Econ. and Social Affairs, Popul. Div., New York. [Available at http://www.un.org/esa/population/publications/WUP2005/2005WUPHighlights_Exec_Sum.pdf]

Vonk, G., S. Geertman, and P. Schot (2007), A SWOT analysis of planning support systems, *Environ. Plan. A*, *39*, 1699–1714, doi:10.1068/a38262.

Wang, X. Y., A. G. Barnett, W. Hu, and S. Tong (2009), Temperature variation and emergency hospital admissions for stroke in Brisbane, Australia, 1996–2005, *Int. J. Biometeorol.*, *53*, 535–541, doi:10.1007/s00484-009-0241-4.

Xu, J., Q. Wei, X. Huang, X. Zhu, and G. Li (2010), Evaluation of human thermal comfort near urban waterbody during summer, *Build. Environ.*, *45*, 1072–1080, doi:10.1016/j.buildenv.2009.10.025.

B. G. Heusinkveld, A. A. M. Holtslag, S. Koopmans, G. J. Steeneveld, and L. W. A. van Hove, Meteorology and Air Quality Section, Wageningen University, PO Box 47, NL-6700 AA Wageningen, Netherlands. (gert-jan.steeneveld@wur.nl)